Transmission Coefficient of an Electron through a Heterostructure with Nanometer-Thick Trapezoidal Barrier Grown on Anisotropic Materials

Lilik Hasanah[1)], Fatimah A.Noor, Khairurrijal, Mikrajuddin, Toto Winata, and Sukirno

[1)] Department of Physics, Institut Teknologi Bandung, Jalan Ganesha 10, Bandung 40132

Abstract

Transmission coefficient of an electrons incident on a heterostructure potential with nanometer-thick trapezoidal barrier grown on anisotropic materials are derived by solving the effective-mass equation including off-diagonal effective-mass tensor elements. The boundary condition for an electron wave function (under the effective-mass approximation) at a heterostructure anisotropic junction is suggested and included in the calculation. The analytic expressions are applied to the Si(110)/$Si_{0.5}Ge_{0.5}$/Si(110) heterostructure, in which the SiGe barrier thickness is several nanometers. It is assumed that the direction of propagation of the electrons makes an arbitrary angle with respect to the interfaces of the heterostructure and the effective mass of the electron is position dependent. The transmission coefficient calculated for energy below the barrier height and varying the applied voltage to the barrier. The transmission coefficient depends on the valley where the electron belongs and not symmetric with the incidence angle.

1. Introduction

Since last half century, the tunneling phenomenon through a potential barrier is still of interest in the study of quantum transport in heterostructures. Paranjape (1995) studied transmission coefficient of an electron in an isotropic heterostructure with different effective masses[1]. Kim and Lee (1998) derived transmission coefficient of an electron tunneling through a heterostructure barrier grown on anisotropic materials by solving the effective-mass equation including off-diagonal effective-mass tensor elements[2],[3]. The effects of different effective masses for a heterostructure junction are also included but they did not consider the effects of voltage applied to the barrier in which the square barrier becomes trapezoidal one. In this paper, we calculate the transmission coefficient of an electron tunneling through a heterostructure with a nanometer-thick trapezoidal barrier grown on an anisotropic material.

2. Theoretical Model

The conduction band energy diagram of a heterostructure is shown in Fig 1 with the potential profile is expressed as :

$$V(z) = \begin{cases} 0 & for \quad z \le 0 \\ \Phi - \dfrac{eV_b}{d} z & for \quad 0 < z < d \\ -eV_b & for \quad z \ge d. \end{cases} \tag{1}$$

Here, the barrier width and height are d and Φ, respectively. The voltage applied to the barrier is V_b with e is the electronic charge. The electron is incident from region I to the potential barrier (region II), in which the material of the region I is the same as that of the material III.

The Hamiltonian for general anisotropic materials is [2]

$$H = \frac{1}{2m_o}\mathbf{p}^T\alpha(\mathbf{r})\mathbf{p} + V(\mathbf{r}), \tag{2}$$

where m_o is the mass of free electron, **p** is the momentum vector, $(1/m_o)\alpha$ is the inverse effective-mass tensor and $V(\mathbf{r})$ is the potential energy. The effective mass of the electron and potential are dependent only on the z direction. The wave function of the effective-mass equation with the Hamiltonian is Eq. (2) is given as [2]:

$$\psi(\mathbf{r}) = \varphi(z)\exp(-i\gamma z)\exp(i(k_x x + k_y y)), \tag{3}$$

and $$\gamma = \frac{k_x\alpha_{xz} + k_y\alpha_{yz}}{\alpha_{zz}} \tag{4}$$

is wave number parallel to the interface.

By employing the separation variable to Eq. (2), it is easily found that $\varphi(z)$ satisfies the one dimensional Schrödinger-like equation:

$$-\frac{\hbar^2}{2m_o}\alpha_{zz,l}\frac{\partial^2\varphi(z)}{\partial z^2} + V(z)\varphi(z) = E_z\varphi(z), \tag{5}$$

where $\hbar$ is the reduced Planck constant, the subscript l in $\alpha_{zz,l}$ denotes each region in Fig. 1 and

$$E_z = E - \frac{\hbar^2}{2m_o}\sum_{i,j\in\{x,y\}}\beta_{ij}k_i k_j . \tag{6}$$

Here

$$E = \sum_{i,j\in\{x,y,z\}}\frac{\hbar^2}{2mo}\alpha_{ij,1}k_i k_j \tag{7}$$

is the total energy,

$$\beta_{ij} = \alpha_{ij} - \frac{\alpha_{iz}\alpha_{zj}}{\alpha_{zz}}, \tag{8}$$

and α_{ij} is the effective mass tensor element.

The time-independent electron wave function in each region is therefore:

$$\Psi_1(z) = (Ae^{ik_1 z} + Be^{-ik_1 z})e^{-(i\gamma_1 z)}e^{-(ik_x x + ik_y y)}, \qquad \text{for } z \le 0, \qquad (9)$$

$$\Psi_2(z) = (Ce^{-\int_0^z k_2(z)dz} + De^{\int_0^z k_2(z)dz})e^{-(i\gamma_2 z)}e^{-(ik_x x + ik_y y)}, \qquad \text{for } 0 < z < d, \qquad (10)$$

$$\Psi_3(z) = Fe^{ik_3 z}e^{-(i\gamma_1 z)}e^{-(ik_x x + ik_y y)}. \qquad \text{for } z \ge d. \qquad (11)$$

The incident wave $A\exp(ik_1 z)$ has the wave number k_1 which is given as :

$$k_1 = \left\{ \frac{2m_o E_z}{\hbar^2} \frac{1}{\alpha_{zz,1}} \right\}^{1/2}, \qquad (12)$$

where E_z is smaller than the barrier height Φ. The wave numbers $k_2(z)$ and k_3 are expressed, respectively, as follows

$$k_2(z) = \left\{ \frac{2m_0}{\hbar^2} \frac{1}{\alpha_{zz,2}} (\Phi - e\frac{V_b}{d} z) - \frac{\alpha_{zz,1}}{\alpha_{zz,2}} k_1^2 - \frac{1}{\alpha_{zz,2}} \sum_{i,j \in (x,y)} (\beta_{ij,1} - \beta_{ij,2}) k_i k_j \right\}^{1/2}, \qquad (13)$$

and

$$k_3 = \left\{ \frac{2m_o (E_z + eV_b)}{\hbar^2} \frac{1}{\alpha_{zz,1}} \right\}^{1/2}. \qquad (14)$$

By applying the boundary conditions at z = 0 dan z = d, which are expressed as follows [3]:

$$\psi_I(z = 0^-) = \psi_2(z = 0^+), \qquad (15a)$$

$$\frac{1}{m_o}\left[\alpha_{zx,I} \frac{d\psi_1}{dz} + \alpha_{zy,I} \frac{d\psi_1}{dz} + \alpha_{zz,I} \frac{d\psi_1}{dz} \right]_{z=0^-}$$

$$= \frac{1}{m_o}\left[\alpha_{zx,2} \frac{d\psi_2}{dz} + \alpha_{zy,2} \frac{d\psi_2}{dz} + \alpha_{zz,2} \frac{d\psi_2}{dz} \right]_{z=0^+}, \qquad (15b)$$

$$\psi_2(z = d^-) = \psi_3(z = d^+), \qquad (15c)$$

$$\frac{1}{m_o}\left[\alpha_{zx,2}\frac{d\psi_2}{dz}+\alpha_{zy,2}\frac{d\psi_2}{dz}+\alpha_{zz,2}\frac{d\psi_2}{dz}\right]_{z=d^-}$$

$$=\frac{1}{m_o}\left[\alpha_{zx,1}\frac{d\psi_3}{dz}+\alpha_{zy,1}\frac{d\psi_3}{dz}+\alpha_{zz,1}\frac{d\psi_3}{dz}\right]_{z=d^+}, \tag{15d}$$

we obtain the transmission amplitude T_a from Eqs. (9) and (11) which can be written as:

$$T_a=\frac{F}{A}=G\exp(i\phi)\,. \tag{16}$$

Here,

$$G=\frac{2k_1k_2^d}{(P^2Sinh^2(u)+Q^2Cosh^2(u))^{1/2}} \tag{17}$$

is the magnitude of T_a,

$$\phi=\left[\tan^{-1}\left(\frac{P}{Q}\right)\tanh(u)\right]-k_3d+(\gamma_1-\gamma_2)d \tag{18}$$

is the phase of T_a,

$$P=(\frac{\alpha_{zz,1}}{\alpha_{zz,2}}k_1k_3-\frac{\alpha_{zz,2}}{\alpha_{zz,1}}k_2^0k_2^d)\,, \tag{19}$$

$$Q=(k_3k_2^0+k_1k_2^d)\,, \tag{20}$$

$$k_2^0=k_2(z=0)\,, \tag{21}$$

$$k_2^d=k_2(z=d)\,, \tag{22}$$

and $u=\int_0^d k_2(z)dz\,.$ (23)

The transmission coefficient is easily obtained from Eq. (16) by employing the expression :

$$T=T_a^{*}T_a \tag{24}$$

If the voltage applied to the barrier is zero, then $k_2^0 = k_2^d = k_2$ dan $k_1 = k_3$, and the expressions in Eqs. (17) and (18) will be the same as that given by Lee [2], in which

$$G = \frac{2k_1k_2}{(P^2 Sinh^2(u) + Q^2 Cosh^2(u))^{1/2}}, \tag{25}$$

$$\phi = \left[\tan^{-1}\left(\frac{P}{Q}\right)\tanh(u)\right] - k_3 d + (\gamma_1 - \gamma_2)d, \tag{26}$$

$$P = \left(\frac{\alpha_{zz,I}}{\alpha_{zz,2}}k_1^2 - \frac{\alpha_{zz,2}}{\alpha_{zz,I}}k_2^2\right), \tag{27}$$

$$Q = 2k_1k_2, \tag{28}$$

and $u = k_2 d$. (29)

3. Calculated Results and Discussion

The model used in the numerical calculation is shown in Fig. 1. There is a strained $Si_{0.5}Ge_{0.5}$ potenstial barrier grown on Si (110). The width of the barrier d is 50 Å and the band discontinuity Φ is taken as 216 meV.

There are four equivalent valleys in the conduction band of Si(110) with a strained $Si_{0.5}Ge_{0.5}$ potential barrier. The effective mass tensor elements of these four valley are not the same. There are two groups of valleys in Si(110) and $Si_{0.5}Ge_{0.5}$. The inverse effective inverse masses used in our example are related to the tensor elements α_{ij} shown in Table 1 [2].

Figure 2 shows the chosen coordinate system. We take the position where the electron hits the barrier as the origin of the coordinate system. In the spherical coordinate system shown in Fig. 2, Eq. (7) becomes

$$
\begin{aligned}
E = \frac{\hbar^2}{2m_o}\Big\{ & \alpha_{xx1}k^2\sin^2\theta\cos^2\varphi + \alpha_{yyx1}k^2\sin^2\theta\sin^2\varphi + \alpha_{zz1}k^2\cos^2\theta \\
& + 2\big(\alpha_{xy1}k^2\sin^2\theta\cos\varphi\sin\varphi + \alpha_{yz1}k^2\sin^2\theta\cos\theta\sin\varphi \\
& + \alpha_{zx1}k^2\sin^2\theta\cos\theta\cos\varphi\big)\Big\} \quad . \qquad (30)
\end{aligned}
$$

We calculated the transmission coefficient for the angle of incidence for **k** (the wave vector of incident electron) varying from -90^o to 90^o with incident energies are 25 meV, 75 meV and 150 meV and varying the applied voltage from 50 mV to 150 mV. The incidence angles are θ dan φ, but we fix φ to π/2 for simplicity and change only θ.

The numerical value of transmission coefficient with incident energy of 75 meV and applied voltage of 50 mV is shown in Fig. 3. Valley 1 and valley 2 have the biggest values of transmission coefficient is at normal incidence. We also see that, for all valley, the transmission coefficient is not symmetric with the incidence angle.

In Fig. 4 we have given the numerical value of transmission coefficients with incident energy of 150 meV and applied voltage of 50 mV. Valley 1 and valley 2 have the highest transmission coefficient value at about normal incidence and the transmission coefficient value is higher than for the transmission coefficient with incident energy 75 meV. It is because electron has energy more high to tunnel the barrier. The same with with Fig. 3, for all valleys, the transmission coefficient is not symmetric with the incidence angle.

If we decrease the incident energy, the electron must have lower energy to tunnel the potential barrier so that the probability of tunnelling the barrier must smaller than if electron has higher incident energy as shown in Fig. 5. But for the same incident energy, the transmission coefficient will increase when the applied voltage to the barrier increased as shown in Fig. 6. For case in Figs. 5 and 6, the transmission coefficient is maximum at normal incident. We also see that, in all valleys, the transmission coefficient is not symmetric with the change of sign of incidence angle ($\theta \rightarrow -\theta$), which confirms the anisotropic of the materials [2].

Conclusion

We have derived an analytical expression of transmission coefficients of electron through a nanometer-thick trapezoidal barrier grown on anisotropic materials under non-normal incidence. We included the effect of different effective masses at heterojunction interfaces. The boundary condition for an electron wave function (under the effective-mass approximation) at a heterostructure anisotropic junction is suggested and included in the calculation. The calculation is done with a $Si_{0.5}Ge_{0.5}$ potential barrier grown on Si (110). The transmission coefficient will increase if the incident energy is increased. For the same incident energy, the biggest value of the transmission coefficient happens if the applied voltage to the barrier is high. The calculation shows that the transmission coefficient and the tunneling time depend on the valley and it is not symmetric with the angle of incidence.

Reference:

[1] V.V. Paranjape: Transmission coefficient and stationary-phase tunneling time of an electron through a heterostructure, *Phys.Rev. B*. Vol 52. No 15, 1995, 10 740-10 743

[2] K.-Y. Kim and B. Lee: Transmission coefficient of an electron through a heterostructure barrier grown on anisotropic materials, *Phys.Rev. B*. Vol 58. No 11, 1998, 6728-6731

[3] K.-Y. Kim and B. Lee: Tunneling time and the post-tunneling position of an electron through a potential barrier in an anisotropic semiconductor, *Superlattice Microstruct*. Vol 24. No 6, 1998, 389-397

[4] Khairurrijal, F. A. Noor, and Sukirno, “Electron direct tunneling time in heterostructure with nanometer-thick trapezoid barriers” *Solid-State Electronics*, vol. 49, no. 6, pp. 923-927, 2005.

[5] B. Lee and W. Lee: Electron tunneling through a potential barier under non-normal incidence, *Superlattice Microstruct*. Vol 18. No 3, 1995, 177-185

Table1. Tensor elements (α_{ij}) used in the numerical calculation.

Valley	Region I dan III (Si [110])	Region II ($Si_{0,5}Ge_{0,5}$)
1	$\begin{matrix} 5.26 & 0 & 0 \\ 0 & 3.14 & 2.12 \\ 0 & 2.12 & 3.14 \end{matrix}$	$\begin{matrix} 6.45 & 0 & 0 \\ 0 & 4.56 & 2.74 \\ 0 & 2.74 & 4.56 \end{matrix}$
2	$\begin{matrix} 5.26 & 0 & 0 \\ 0 & 3.14 & -2.12 \\ 0 & -2.12 & 3.14 \end{matrix}$	$\begin{matrix} 6.45 & 0 & 0 \\ 0 & 4.56 & -2.74 \\ 0 & -2.74 & 4.56 \end{matrix}$

Table 1. L. Hasanah, et.al.

FIGURE CAPTIONS

Figure 1. The potential profile of a heterostructure without a bias voltage (a) and with the application of a voltage to the barrier

Figure.2. The coordinates used in the analysis

Figure 3. The transmission coefficient for the angle of incident varying from -90^o to 90^o with incident energies of 75 meV and applied voltage of 50 mV

Figure 4. The transmission coefficient for the angle of incident varying from -90^o to 90^o with incident energies of 150 meV and applied voltage of 50 mV

Figure 5. The transmission coefficient for the angle of incident varying from -90^o to 90^o with incident energies of 25 meV and applied voltage of 100 mV

Figure 6. The transmission coefficient for the angle of incident varying from -90^o to 90^o with incident energies of 25 meV and applied voltage of 150 mV

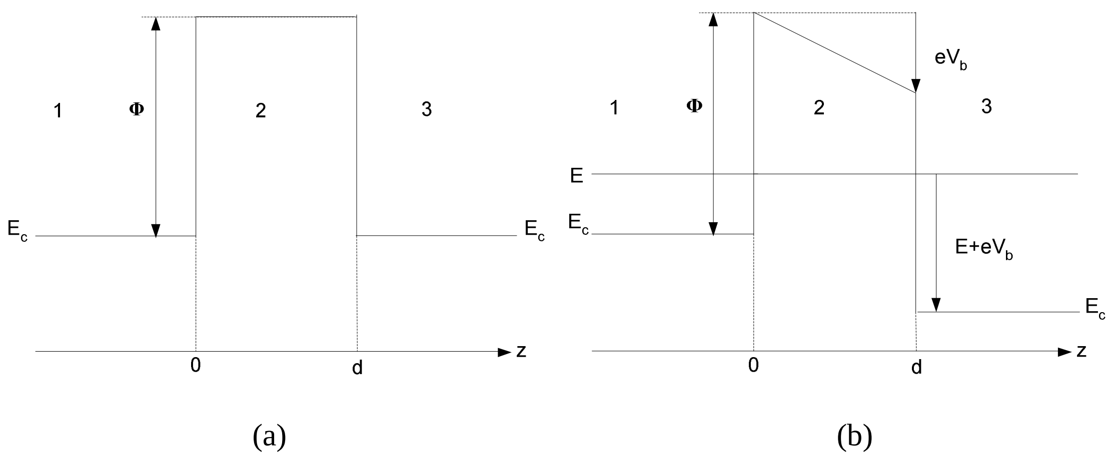

Fig.1 L. Hasanah, et.al.

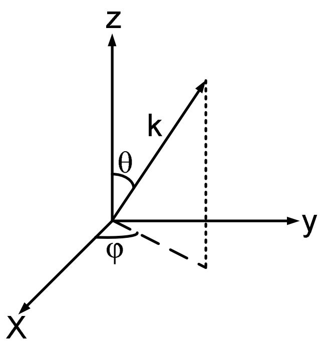

Fig.2 L. Hasanah, et.al.

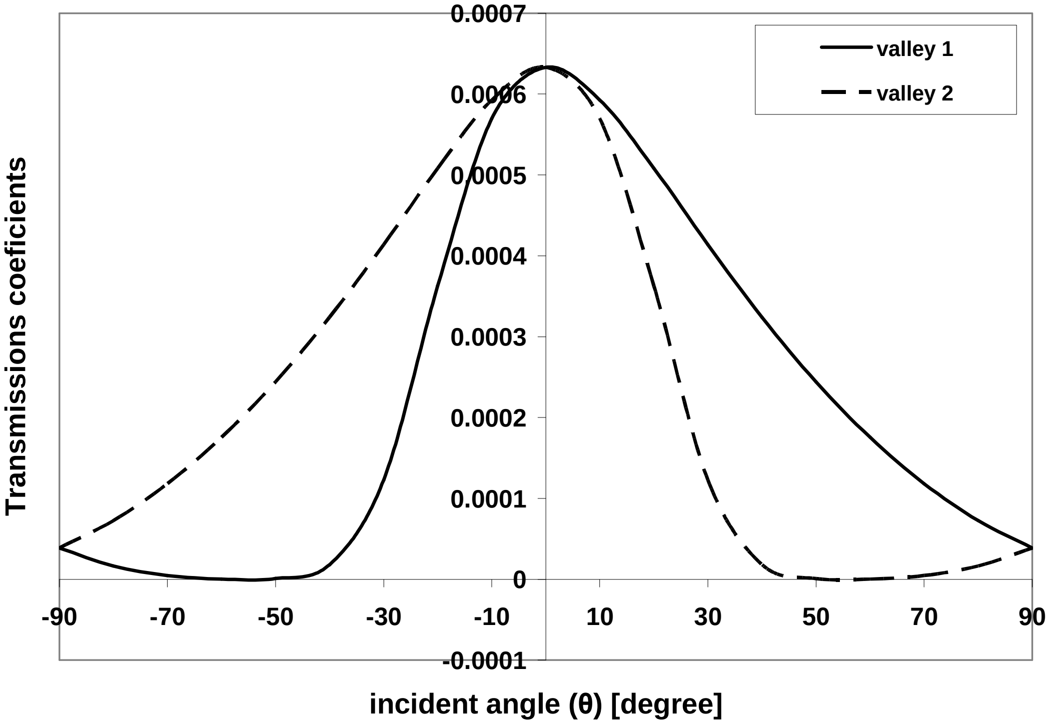

Fig.3 L. Hasanah, et.al.

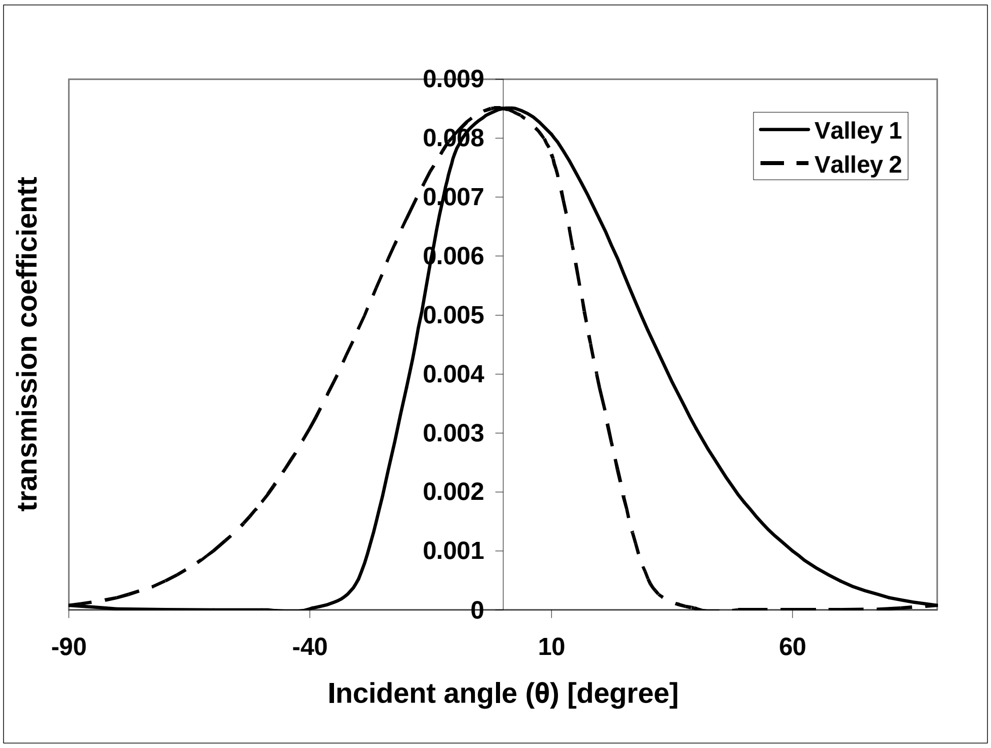

Fig.4 L. Hasanah, et.al.

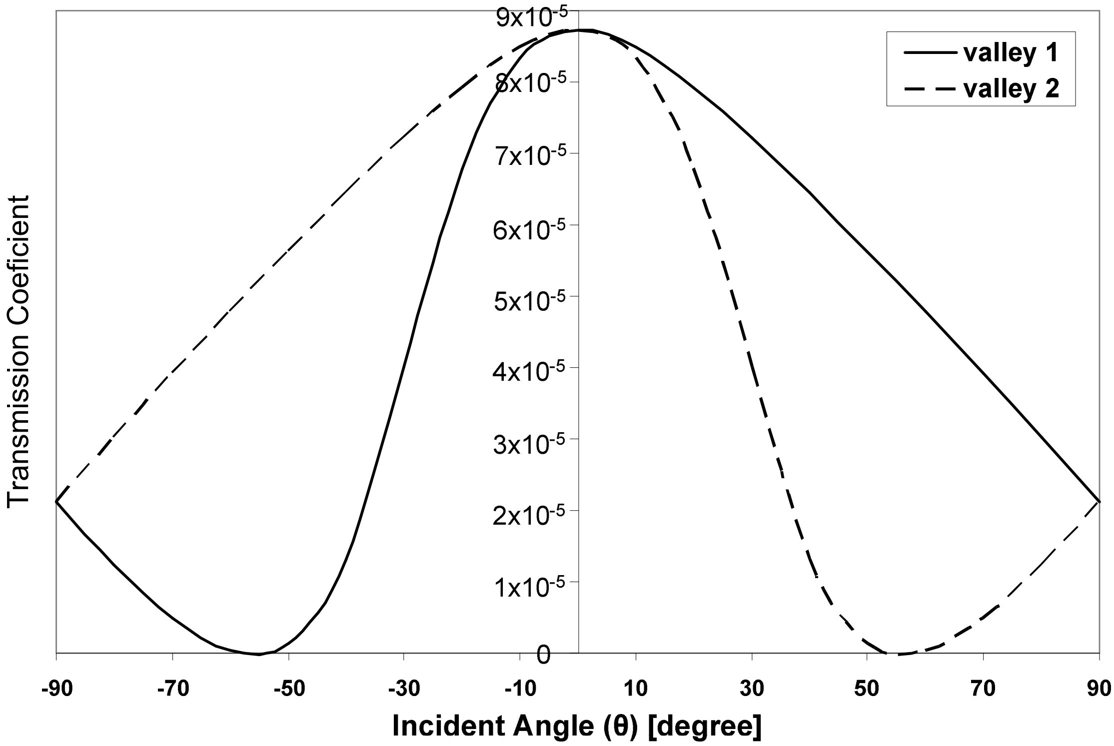

Fig.5 L. Hasanah, et.al.

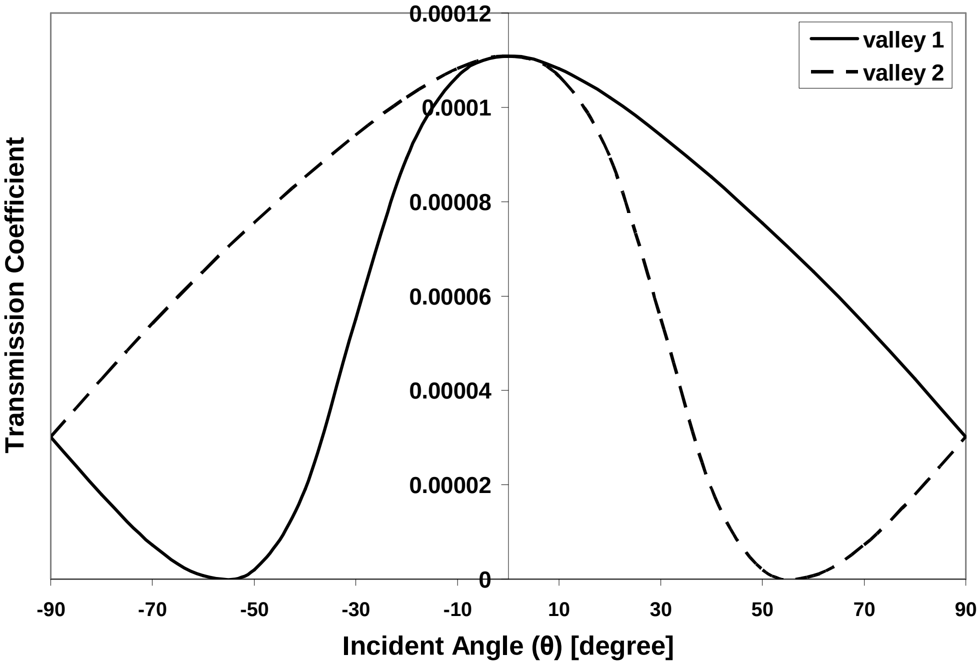

Fig.6 L. Hasanah, et.al.